allow the measurement of long phonon lifetimes and high quality factors. Furthermore, it opens the door to the design of experiments with a known and controlled phonon population. □

Received 7 June; accepted 20 September 2004; doi:10.1038/nature03046.

1. Park, H. *et al.* Nanomechanical oscillations in a single-C_{60} transistor. *Nature* **407,** 57–60 (2000).
2. Pasupathy, A. N. *et al.* Vibration-assisted electron tunneling in C_{140} single-molecule transistors. Preprint at ⟨http://arxiv.org/cond-mat/0311150⟩ (2003).
3. Park, J. *et al.* Coulomb blockade and the Kondo effect in single-atom transistors. *Nature* **417,** 722–725 (2002).
4. Zhitenev, N. B., Meng, H. & Bao, Z. Conductance of small molecular junctions. *Phys. Rev. Lett.* **88,** 226801 (2002).
5. Qiu, X. H., Nazin, G. V. & Ho, W. Vibronic states in single molecule electron transport. *Phys. Rev. Lett.* **92,** 206102 (2004).
6. Weig, E. M. *et al.* Single-electron-phonon interaction in a suspended quantum dot phonon cavity. *Phys. Rev. Lett.* **92,** 046804 (2004).
7. Stipe, B. C., Rezaei, M. A. & Ho, W. Single-molecule vibrational spectroscopy and microscopy. *Science* **280,** 1732–1735 (1998).
8. LeRoy, B. J., Lemay, S. G., Kong, J. & Dekker, C. Scanning tunneling spectroscopy of suspended single-wall carbon nanotubes. *Appl. Phys. Lett.* **84,** 4280–4282 (2004).
9. Grabert, H. & Devoret, M. H. *Single Charge Tunneling* (Plenum, New York, 1992).
10. Liang, W. J., Bockrath, M. & Park, H. Shell filling and exchange coupling in metallic single-walled carbon nanotubes. *Phys. Rev. Lett.* **88,** 126801 (2002).
11. Cobden, D. H. & Nygard, J. Shell filling in closed single-wall carbon nanotube quantum dots. *Phys. Rev. Lett.* **89,** 046803 (2002).
12. Venema, L. C., Meunier, V., Lambin, Ph. & Dekker, C. Atomic structure of carbon nanotubes from scanning tunneling microscopy. *Phys. Rev. B* **61,** 2991–2996 (2000).
13. Dresselhaus, M. S. & Eklund, P. C. Phonons in carbon nanotubes. *Adv. Phys.* **49,** 705–814 (2000).
14. Vitali, L. *et al.* Phonon spectromicroscopy of carbon nanostructures with atomic resolution. *Phys. Rev. Lett.* **93,** 136103 (2004).
15. Iliev, M. N., Litvinchuk, A. P., Arepalli, S., Nikolaev, P. & Scott, C. D. Fine structure of the low-frequency Raman phonon bands of single-wall carbon nanotubes. *Chem. Phys. Lett.* **316,** 217–221 (2000).
16. Reulet, B. *et al.* Acoustoelectric effects in carbon nanotubes. *Phys. Rev. Lett.* **85,** 2829–2832 (2000).
17. Cleland, A. *Foundations of Nanomechanics* (Springer, Berlin, 2003).
18. Tien, P. K. & Gordon, J. P. Multiphoton process observed in the interaction of microwave fields with the tunneling between superconductor films. *Phys. Rev.* **129,** 647–651 (1963).
19. Hanna, A. E. & Tinkham, M. Variation of the Coulomb staircase in a two-junction system by fractional electron charge. *Phys. Rev. B* **44,** 5919–5922 (1991).

Acknowledgements We thank Ya. M. Blanter for discussions, and NWO and FOM for funding.

Competing interests statement The authors declare that they have no competing financial interests.

Correspondence and requests for materials should be addressed to C.D. (dekker@mb.tn.tudelft.nl).

Random quasi-phase-matching in bulk polycrystalline isotropic nonlinear materials

M. Baudrier-Raybaut[1], R. Haïdar[1], Ph. Kupecek[1,2], Ph. Lemasson[3] & E. Rosencher[1,4]

[1]*DMPH and DOTA/ONERA, Office National d'Etudes et de Recherches Aérospatiales, Chemin de la Hunière, 91761 Palaiseau, France*
[2]*Université Pierre et Marie Curie, 5 Place Jussieu, Paris 75005, France*
[3]*LPSC/CNRS, 1 Place Aristide Briand, F-92195, France*
[4]*Département de Physique, Ecole Polytechnique, 91228 Palaiseau, France*

Three-wave mixing in nonlinear materials—the interaction of two light waves to produce a third—is a convenient way of generating new optical frequencies from common laser sources. However, the resulting optical conversion yield is generally poor, because the relative phases of the three interacting waves change continuously as they propagate through the material[1]. This phenomenon, known as phase mismatch, is a consequence of optical dispersion (wave velocity is frequency dependent), and is responsible for the poor optical conversion potential of isotropic nonlinear materials[2]. Here we show that exploiting the random motion of the relative phases in highly transparent polycrystalline materials can be an effective strategy for achieving efficient phase matching in isotropic materials. Distinctive features of this 'random quasi-phase-matching' approach are a linear dependence of the conversion yield with sample thickness (predicted in ref. 3), the absence of the need for either preferential materials orientation or specific polarization selection rules, and the existence of a wavelength-dependent resonant size for the polycrystalline grains.

Much effort has recently been devoted to the development of materials which are suitable for nonlinear optical frequency conversion from the near- to the mid-infrared regions[4–7]. Many semiconductor (GaAs, ZnSe, …) materials of space group $\bar{4}3m$ are excellent candidates: they are widespread and mature optoelectronics graded materials, they are transparent in the mid-infrared and they display particularly high nonlinear 2nd-order susceptibilities (that is, for three-wave interaction). In single-crystalline materials, the main factor for an efficient optical conversion is the coherence length Λ_c, the distance over which the relative phase lag of the three waves add up to π. Indeed, because of the different relative phase velocities between the three interacting waves, optical power flows back and forth from the converted waves towards the pumping waves (that is, backconversion) as soon as the interacting distance becomes larger than the coherence length (see Fig. 1). Phase-matching is thus obtained when the coherence length is much longer than the interaction distance in the material. Because of the lack of optical birefringence, such a situation cannot be obtained naturally in isotropic $\bar{4}3m$ semiconductors over long distance. Instead, so-called quasi-phase-matching scenarios based on epitaxial growth on patterned substrates need to be developed[1,8–10].

The backconversion process results from an interference effect between the three coherent waves. Such interference could be destroyed if the waves were allowed to lose their respective phases randomly in the material, in that the nonlinear susceptibility does not average to zero. Such parametric interactions in disordered media have attracted considerable attention in recent years, with a particular emphasis on the nonlinear diffusion/scattering processes[11–14]: In these studies, the average size of the nanocrystal-

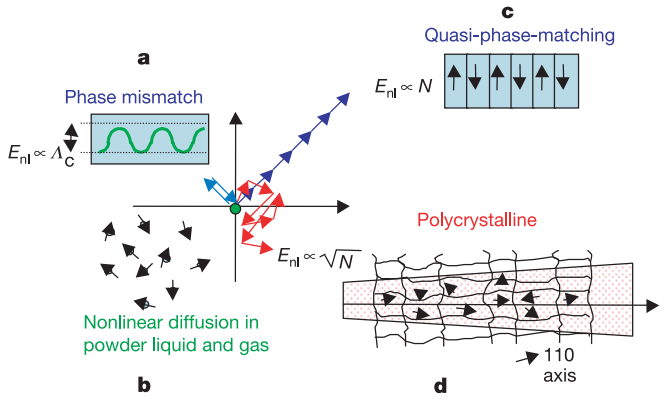

Figure 1 Three-wave mixing mechanisms in bulk, powder, periodically poled and polycrystalline materials. In bulk nonlinear optical materials, the relative phase of the three interacting fields grows continuously with the propagating distance, gaining a phase lag of π every coherence length Λ_c. The transfer of energy between the waves thus oscillates with a period of $2\Lambda_c$, leading to a small (if not null) conversion efficiency (**a**). In quasi-phase-matched materials[10], the orientation of the crystal is rotated every Λ_c, compensating the phase lag of π so that the energy transfer E_{nl} adds up constructively with the propagating distance ($E_{nl} \propto N$, where N is the number of grains) (**c**). In a totally disordered material (powder, gas, liquid), each particle behaves independently, scattering the nonlinearly generated fields in an incoherent way (**b**). In polycrystalline materials, the relative phase diffuses in phase space, leading to a coherent growth of the nonlinear generated fields according to $E_{nl} \propto \sqrt{N}$.

lites is smaller than the interacting wavelengths (Rayleigh regime) so that the samples are highly diffusive and mostly opaque. We show that a similar (but different) strategy can be implemented in polycrystalline ZnSe materials, for which highly transparent materials and controllable grain size are available. The concept of random quasi-phase-matching is experimentally demonstrated in a difference frequency generation (DFG) experiment—a particularly interesting situation which involves large coherence lengths—with emphasis on the influence of the grain size, light polarization and length of the sample, suggesting the potential for new optical random materials[15]. We thus show that a signal far higher than the contribution of a single coherence length can be obtained, as a result of phase randomization due to the random distribution of the microcrystallite ('grain') domains[3] (see Fig. 1).

We first theoretically describe the DFG process in polycrystalline materials. Let E_1^n be the value of the electromagnetic field at the output of the nth grain crossed by the two undepleted laser beams E_2 and E_3. By integration over each grain of size X_m (with a gaussian distribution around its mean value) and summation of all the contributions, as already suggested by refs 3 and 13, the value of E_1^n is deduced from the classical growing term[2], taking into account randomizing phase-distribution terms:

$$E_1^n = \frac{\omega_1}{n_1 c} E_3 E_2^* \sum_{m=1}^{n} d_m \frac{e^{-i\Delta k X_m} - 1}{\Delta k} e^{-i\Delta k \sum_{j=1}^{m-1} X_j} \qquad (1)$$

where c is the velocity of light, E_1, E_2, E_3 designate the DFG and the pump-wave fields of respective angular frequencies ω_1, ω_2 and ω_3, n_1, n_2, n_3 are the optical indexes of the polycrystalline materials for the three waves, $\Delta k = k_3 - k_1 - k_2$ is the phase mismatch wavevector between the three waves in each grain and d_m is the nonlinear coefficient of the mth grain. Numerical simulations show that the term

$$e^{-i\Delta k \sum_{j=1}^{m-1} X_j}$$

in equation (1) is such that, after a few grains, the three waves display a random relative phase while entering each micro-crystal of random size X. This is a key element for the success of random quasi-phase-matching. Performing an ensemble average of the square modulus of equation (1)—meaning that the beam waist is far larger than the mean grain size—the total DFG intensity generated by N grains is then given by:

$$I_1^{\text{poly}} = \frac{8\pi^2}{\lambda_1^2} Z_0 \frac{\langle |d|^2 \rangle}{n_1 n_2 n_3} \langle X^2 \operatorname{sinc}^2(\Delta k X/2) \rangle N I_2 I_3 \qquad (2)$$

where Z_0 is the vacuum impedance (377 Ω) and λ_1 is the wavelength of field E_1. The $\langle x \rangle$ notation designates the mean value of random variable x averaged over its probability distribution $p(x)$. For instance, $\langle |d|^2 \rangle$ is the norm of the effective nonlinear coefficient $\langle |d|^2 \rangle = \int |d(\theta,\varphi)|^2 \, p(\theta,\varphi) \, d\theta \, d\varphi$ averaged over all the possible orientations of the grains (θ and φ are the eulerian coordinates of the grain). More specifically, we made the assumption that the grain size obeys a gaussian distribution, that is, $p(X) = \frac{1}{\sqrt{2\pi}\sigma_x} e^{-(X-\Lambda)^2/2\sigma_x^2}$ where Λ and σ_x are the mean value and the standard deviation of the grain size X respectively. Equation (2) can be written as:

$$I_1^{\text{poly}} = N_{\text{eff}} I_1^{\text{coh}} \qquad (3)$$

where $I_1^{coh} = \frac{32}{\lambda_1^2} Z_0 \frac{|d|^2}{n_1 n_2 n_3} \Lambda_c^2 I_2 I_3$ is the DFG intensity generated by a single coherence length of the materials for the specific three-wave combination, Λ_c is the coherence length and N_{eff} is the effective number of grains participating to the DFG process, given by:

$$\begin{aligned} N_{\text{eff}} &= N \frac{\langle |d|^2 \rangle}{d^2} \langle \sin^2(\Delta k X/2) \rangle \\ &= N \frac{\langle |d|^2 \rangle}{d^2} \frac{1}{\sqrt{2\pi}\sigma_x} \int_0^\infty \sin^2(\Delta k X/2) e^{-(X-\Lambda)^2/2\sigma_x^2} \, dX \end{aligned} \qquad (4)$$

Equations (2)–(4) are very predictive. First, as already predicted in somewhat similar situations[3,13,16], a linear variation of the DFG signal as a function of the sample thickness L (where $L = N\Lambda$) is expected, instead of a quadratic variation for perfect phase matching[1]. We call this regime random quasi-phase-matching (see Fig. 1). Second, the DFG signal never averages to zero whatever the grain orientation distribution. Finally, a careful examination of equation (4) shows that a resonance of the DFG yield is expected once the condition $\Delta k \Lambda = \pi$ is obtained, that is, when the average grain size is close to the DFG coherence length.

The starting polycrystalline ZnSe materials were provided by II–VI, Inc. It consists of micrograins with an average size of $\Lambda = 30\,\mu m$, and a mean standard deviation $\sigma_x \approx 5\%\,\Lambda$. No important crystalline texture is revealed by X-ray Bragg diffraction studies, so that the $\langle |d|^2 \rangle / d^2$ averages to 0.14 (d is the ZnSe nonlinear susceptibility in the $\langle 110 \rangle$ direction and for all the polarization configurations of the interactive waves)[17]. Samples were submitted to a solid phase recrystallization[18] process. Four different mean grain sizes have thus been obtained: 30 μm (unprocessed), 60 μm, 70 μm and 100 μm. The grain size X is also gaussian distributed,

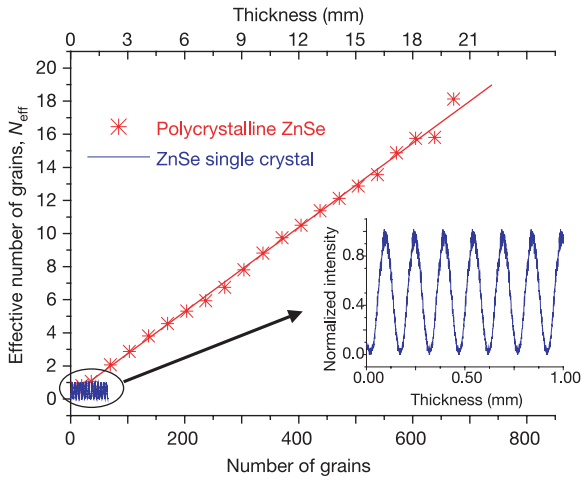

Figure 2 Variation of the normalized DFG intensity I_1 as a function of the polycrystalline sample thickness. The pump wavelengths are 1.925 and 2.380 μm, respectively, yielding a 10-μm generated field. The distance is expressed in terms of the number of ZnSe grains along the optical path ($\Lambda = 30\,\mu m$ in this sample). The DFG signal is normalized to the intensity obtained with a single coherence length in a ZnSe single crystal. The variation of the DFG signal in ZnSe single crystalline materials is shown for comparison. The specificity of random quasi-phase-matching appears clearly.

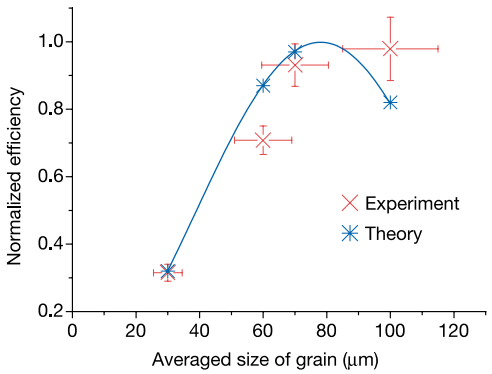

Figure 3 Normalized difference frequency generation efficiency as a function of the ZnSe mean grain size Λ. The different samples are obtained by solid phase recrystallization (straight line, theory; crosses and bars, experimental data points with error bars). A resonant yield appears when the grain size is close to the coherence length (78 μm, in this experimental scheme). Horizontal error bars indicate the standard deviation of the grain size; vertical error bars indicate the standard error of measurement of our experiment.

with a uniform standard deviation of 5 Λ/100. To study the DFG conversion efficiency as a function of the sample thickness L, the samples are bevelled by mechanical polishing to produce wedges with angles of 25° for the recrystallized samples and 37° for the unprocessed ones.

For the DFG experiment, the pump source is a 100-mJ, 30-Hz, 1.06-μm pumped $LiNbO_3$ type I optical parametric oscillator with signal and idler waves tunable between 1.8 and 2.4 μm, yielding an 8–12-μm DFG field. See ref. 19, where a similar set-up has been used to measure DFG coherence length in ZnSe (~78 μm in the 8–12-μm DFG range)[19]. If a resonance is to be found, it is thus expected for a grain size of about 78 μm. This large value of the coherence length originates from the minimum index dispersion of ZnSe in this spectral region equidistant between the gap and the Restrahlung energies. This explains the large nonlinear yields expected in ZnSe polycrystalline materials, as expected from equations (1) to (4). About 200 μJ of the available energy are focused to a waist of about 200 μm in the samples. The bevelled samples are translated on a motorized mount. The DFG wave energy is measured using a HgCdTe cryogenic detector protected by adequate filters.

We first studied the variation of the DFG signal as a function of the sample thickness. To explore a large thickness range, we chose the 37° wedged sample. Figure 2 shows the variation of the measured signal as a function of the crystal thickness. The signal was normalized to the signal obtained in the same configuration by a DFG signal due to a signal coherence length (as determined in a crystalline ⟨110⟩ wedge sample[19]). Clearly, the signal follows the expected linear dependence on sample length L. Given the experimental values $\Lambda/\Lambda_c \approx 0.38$, $\sigma_x/\Lambda \approx 5\%$ and $\langle d^2\rangle/d^2 \approx 14\%$, equation (4) predicts a N_{eff}/N ratio of 4.5%, whereas a ratio of 2.8% is experimentally determined from Fig. 2, which is the right order of magnitude.

We then studied the influence of the grain size on the DFG signal. The preceding experiment was performed for each of the three SPR samples. Linear variations as a function of the sample thickness were observed in all the samples. Figure 3 shows the theoretical and experimental values of the normalized efficiency for the four different values of the grain mean size Λ, taking into account an experimentally determined loss term of $\rho = 4.5\%\ cm^{-1}$. This loss is due to a very small amount of light scattering (corresponding to a mean free path for ~2-μm photons of 22 cm), a situation which is fundamentally different from previous work[14]. The observed variations are in good agreement with the theoretical predictions. Finally, we study the variation of the DFG signal as a function (1) of the orientation of the pump polarization relative to the sample bevel direction, (2) of the angle between the pump and the DFG beam polarization, and (3) of the two pump frequencies. No significant variation of the DFG signal could be observed in any of these experiments, which confirms the absence of crystallographic texture in our samples.

Random quasi-phase-matching may then become a valuable building block in nonlinear optics. Such materials can be deposited on any substrate (such as silicon) with no particular restrictions regarding crystalline growth or sample length, opening the way to optical conversion in low-cost deposited waveguides. Its extremely loose frequency selectivity makes it of particular interest for generating optical radiations with ultra-wide spectral tunability and reasonable efficiency. It may also be applied to emerging materials such as ZnO, chromium-doped ZnSe or new laser ceramics, allowing multifunctional materials to be developed.

We note that, although quasi-phase-matched GaAs crystals have been demonstrated to be far more efficient nonlinear optical converters in the 8–12 μm range[8,9,20], these crystals have not yet been demonstrated over large lengths. But large size samples are available in polycrystalline materials (commonly > 100 mm for the ZnSe samples), so that good conversion yields could eventually be reached. This, added to the extreme ease-of-use of the random quasi-phase-matching technique (almost no control is needed), makes of any piece of polycrystalline ZnSe a cheap and efficient optical converter. □

Received 3 May; accepted 22 September 2004; doi:10.1038/nature03027.

1. Armstrong, J. A., Bloembergen, N., Ducuing, J. & Pershan, P. S. Interactions between light waves in a nonlinear dielectric. *Phys. Rev.* **127,** 1918–1939 (1962).
2. Rosencher, E. & Vinter, B. *Optoelectronics* (Cambridge Univ. Press, Cambridge, 2002).
3. Morozov, E. Y., Kaminskii, A. A., Chirkin, A. S. & Yusupov, D. B. Second optical harmonic generation in non linear crystals with a disordered domain structure. *JETP Lett.* **73,** 647–650 (2001).
4. Fejer, M. M. Nonlinear optical frequency conversion. *Phys. Today* **40,** 25–32 (1994).
5. Ebrahimzadeh, M. & Dunn, M. H. Parametric generation of tunable light from continuous-wave to femtosecond pulses. *Science* **286,** 1513–1517 (1999).
6. Fiore, A., Berger, V., Rosencher, E., Bravetti, P. & Nagle, J. Phase matching using an isotropic nonlinear optical material. *Nature* **391,** 463–466 (1998).
7. Rosencher, E. *et al.* Quantum engineering of optical nonlinearities. *Science* **271,** 168–173 (1996).
8. Levi, O. *et al.* Difference frequency generation of 8-μm radiation in orientation-patterned GaAs. *Opt. Lett.* **27,** 2091–2093 (2002).
9. Eyres, L. A. *et al.* All-epitaxial fabrication of thick, orientation-patterned GaAs films for nonlinear optical frequency conversion. *Appl. Phys. Lett.* **79** (2001).
10. Fejer, M. M., Magel, G. A., Jundt, D. H. & Byer, R. L. Quasi-phase-matched second harmonic generation: tuning and tolerances. *IEEE J. Quant. Electron.* **28,** 2631–3654 (1992).
11. Agranovitch, V. M. & Kravtsov, V. E. Nonlinear backscattering from opaque media. *Phys. Rev. B* **43,** 13691–13694 (1991).
12. Kravtsov, V. E., Agranovitch, V. M. & Grigorishin, K. I. Theory of second-harmonic generation in strongly scattering media. *Phys. Rev. B* **44,** 4931–4942 (1991).
13. Makeev, E. V. & Skipetrov, S. E. Second harmonic generation in suspensions of spherical particles. *Opt. Commun.* **224,** 139–147 (2003).
14. Mel'nikov, V. A. *et al.* Second-harmonic generation in strongly scattering porous gallium phosphide. *Appl. Phys. B* **79,** 225–228 (2004).
15. Wiersma, D. S. & Cavalieri, S. A temperature-tunable random laser. *Nature* **414,** 708–709 (2002).
16. Kurtz, S. K. & Perry, T. T. A powder technique for the evaluation of non linear optical materials. *J. Appl. Phys.* **39,** 3798–3813 (1968).
17. Shoji, I., Kondo, T., Kitamoto, A., Shirane, M. & Ito, R. Absolute scale of second-order nonlinear-optical coefficients. *J. Opt. Soc. Am. B* **14,** 2268–2294 (1997).
18. Rzepka, E., Roger, J. P., Lemasson, P. & Triboulet, R. Optical transmission of ZnSe crystals grown by solid phase recrystallisation. *J. Cryst. Growth* **197,** 480–484 (1999).
19. Haidar, R. *et al.* Largely tunable mid-infrared (8–12 μm) difference frequency generation in isotropic semiconductors. *J. Appl. Phys.* **91,** 2550–2552 (2002).
20. Vodopyanov, K. L. *et al.* Optical parametric oscillation in quasi-phase-matched GaAs. *Opt. Lett.* **29,** 1912–1914 (2004).

Acknowledgements We are indebted to C. Sanchez and A. Cheniere for X-ray measurements, A. Godard, M. Lefebvre and N. Guérineau for help, to M. Fejer for discussions, and D. Sessler for critical reading of the manuscript. This work was supported by the Délégation Générale pour l'Armement (DGA).

Competing interests statement The authors declare that they have no competing financial interests.

Correspondence and requests for materials should be addressed to E. R. (rosencher@onera.fr).

Metal wires for terahertz wave guiding

Kanglin Wang & Daniel M. Mittleman

Department of Electrical and Computer Engineering, MS 366, Rice University, Houston, Texas 77251-1892, USA

Sources and systems for far-infrared or terahertz (1 THz = 10^{12} Hz) radiation have received extensive attention in recent years, with applications in sensing, imaging and spectroscopy[1–10]. Terahertz radiation bridges the gap between the microwave and optical regimes, and offers significant scientific and technological potential in many fields. However, waveguiding in this intermediate spectral region still remains a challenge. Neither conventional metal waveguides for microwave radiation, nor dielectric fibres for visible and near-infrared radiation can be used to guide terahertz waves over a long distance, owing to the high loss from the finite conductivity of metals or the high